CHARACTERIZATION AND ANALYSES ON RESIDUAL STRESS AND DEFORMATION DISTRIBUTION IN LINE HEAT PROCESS

(DOI No: 10.3940/rina.ijme.2016.a4.380)

B Zhou, School of Naval Architecture and Ocean Engineering, Dalian University of Technology, China, **X Han, W Guo,** and **Z Liu,** Maritime Research Centre, Nanyang Technological University, Singapore, and **S-K Tan** School of Civil and Environmental Engineering, Nanyang Technological University, Singapore

SUMMARY

Line heating is an important plate bending process that has been adopted in shipyards for more than 60 years. This paper presents the results of a numerical and experimental study on the residual deformation and stress distribution in the plate forming process using the line heating method. In this paper, a finite element model was used to simulate the heating process, and the model was validated using experimental results. The model was then used to analyze the deformation and stress distributions in the heating and non-heating region. The impact of line heating and sequence of heating on both sides of a steel plate was discussed. The findings of the study show that the compression stress generated help to increase the shrinkage of line heating process. This study presents a valuable reference for similar thermal process.

1 INTRODUCTION

Residual stresses are common in ship and offshore structures and are results of local plastic deformation from thermal and mechanical operations during the fabrication process. Residual stress is superimposed on stress due to applied load to produce a redistribution of deformation and residual stress, which not only reduces the stiffness and stability of the structure, but also seriously affects the fatigue strength of the structure, brittle fracture resistance capability, the ability to resist stress corrosion cracking and high temperature creep cracking. Therefore, residual stress due to the fabrication is a necessary and important consideration in ship and offshore structures.

There are some commonly adopted thermal processes in the shipbuilding industry, and they include welding and line heating. Many studies about the residual stress of welding process (Radaj, 1992 [11]; Brickstad and Josefson 1998 [1], Teng et al. 2001 [9], Deng 2009 [2]) have been reported. However, there is limited information available on the residual stress distribution attributable to line heating process. Although the method is a popular and efficient technique for forming steel plates for ship hull, and has been used in the shipbuilding industry for more than 60 years, line heating and the residual stress it entails has not been studied comprehensively. Plate forming by line heating is a complex thermal transient process that involves thermodynamics, elastic–plastic mechanics and metallurgy, including material engineering and sciences. Study on the residual stress due to line heating process is timely and essential to add to the body of knowledge on residual stress and the effects on such stress when modern ships are expected to carry more loads, move faster and make responsive maneuver in the sea environment.

Line heating has been investigated analytically, experimentally and numerically. The mechanics of line heating process was conducted studies on to predict the final shape of the metal plate according to the heating conditions and mechanical properties of the plate (Moshaiov and Vorus 1987 [8], Ji and Liu 2001 [3] and Ueda et al. 1994a, 1994b, 1994c [12,13,14]). Heating and cooling processes were designed based on their experience of forming simple surface shape from rectangular plates (Ueda et al. 1994a, 1994b, 1994c [12,13,14] and Liu et al. 2006 [4]). Strain or curvature analysis was employed to design heating lines needed to achieve the desired shape of the plate. Deformation in line heating was predicted using thermo-mechanical models (Jang et al. 1997 [5], Yu 2000 [16], Yu et al. 1999, 2001 [15,16]). The heat flux from line heating was treated as a point source, which resulted in considerable errors in predicting the temperature field (Jang et al. 1997 [5]). Transient analysis was used to investigate the unsteady temperature field in the plate during a flame bending process (Moshaiov and Shin, 1991 [7]). The velocity field from a small gas torch was measured and converted into heat flux (Tomita et al. 2001 [10]). The heat transfer analysis between a heat source and the steel plate was performed to determine the temperature field (Jong and Jong 2003 [6]). A numerical thermo-mechanical model was developed to predict the thermal history and resulting deformation of the heating area (Zhou et al., 2014 [18]). The feasibility of multiple torch process and the effects of heat line spacing are also analyzed (Zhou et al. 2015).

As described above, detailed and accurate stress distributions in the whole steel plate for line heating are not available. The present study using finite element method to perform three dimensional simulations aimed at establishing key parameters for residual stress distribution on the whole steel plate subjected to localized line heating. The numerical model was validated with experimental results.

2. NUMERICAL SIMULATIONS

2.1 NUMERICAL MODEL

Numerical analysis of the line heating process was performed using the software ANSYS. Heat transmission and distribution in the plate subject to line heating process

was deduced indirectly and iteratively using the finite element method. Geometrical dimensions of the steel plate were as follows: length was 3m, width 1.5m, thickness 0.014m, and the radius of curvature was 5m. There were 14 heating lines on both sides of the steel plate (see Figure 1). The length of each heating line was 0.3m and the distance between the heating lines was 0.35m. The heating time of each line was 120 seconds. The heating process was applied from the middle to the edge of steel plate according to the order as shown in Figure 1 from No.1 to No.14. The side of steel plate with heating line No.1 to No.7 was designated as the "Upper Edge", and the other side with heating line No.8 to No.14 was designated as the "Lower Edge".

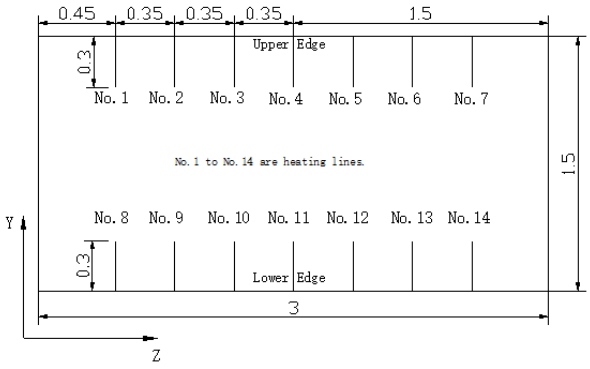

Figure 1. The sketch of heating line arrangement (Unit: m)

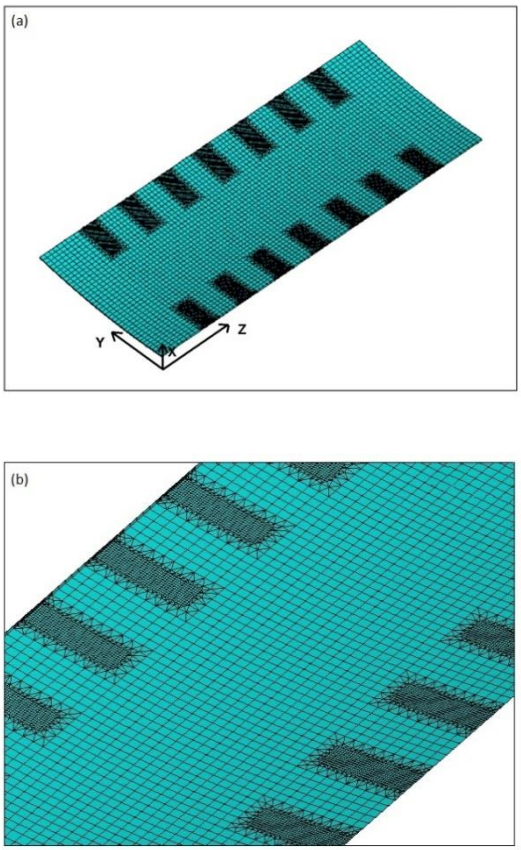

Figure.2. Finite element model of cylinder plate

Figure 2 shows the corresponding finite element model of a cylindrical plate. Fine element mesh size in the line-heated area was used to capture the high temperature gradients. Other areas far from the heated zone were modeled using coarser meshes. The intermediate elements were set up to link the fine and coarse meshes. Several assumptions and choices were made in the formulation of the numerical models, including the perfectly homogeneous and isotropic material, same initial and ambient temperature, heat transferred within the steel plate and between the steel plate and the surrounding air through conduction, convection and thermal radiation. The coordinate system is also shown in Figure 2 (a). The X-axis is along the thickness direction of steel plate, the Y-axis is along the width direction and the Z-axis is along the length direction.

2.2 MATERIAL PROPERTIES

Mild steel plate was considered in this study. Temperature dependent material properties such as thermal conductivity, specific heat, elastic modulus and yield stress were as shown in Figure 3, and were used in the simulation of the transient temperature and deformation distributions [Zhou et al.2009, 2013 [20,21]]. The highest temperature of line heating process was about 850 °C.

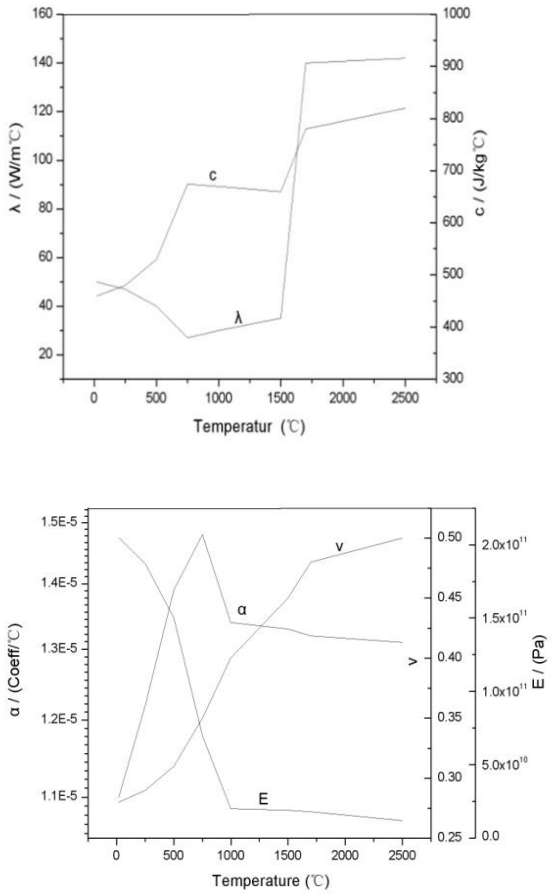

Figure 3. Material properties of carbon steel

2.3 BOUNDARY CONDITIONS

In the thermal analysis, a moving heat source as described by the Gaussian model was used in the finite element simulation of the line-heating process. The water cooling nozzle region was modeled as a trapezoid behind the heat source. Boundary heat transfer between the steel plate and the surrounding air was modeled based on convection and radiation. Surface heat loss was quantitatively much smaller than that due to conduction within the steel plate, which was not critical to the development of the model, and could be ignored. In the mechanical analysis, and to avoid the rigid body movement, boundary conditions were set to zero displacement at endpoints of the metal plate (along the longitudinal axis).

2.4 EXPERIMENTS VALIDATION

Laboratory experiments were carried out to validate the numerical model established in this study, see Figure 4. The dimensions of steel plate and heating condition are the same with numerical analysis. As shown in Figure 4, the temperature field of line heating was measured by Infrared Thermography system. Infrared Thermography system is a convenient, accurate, non-contact method for making temperature field measurement. The temperature distribution can be displayed in a number of different ways. The method that was used to display the data in this analysis was the isothermal contours (regions of equivalent temperature). The temperature fields in the form of isothermal maps measured experimentally and numerically are shown in Figure 5 and Figure 6, respectively. The isothermal contour consists of several bands with increasing temperature from the outer edges to the center of heat line. The isotherm shows an elliptical shape and is denser at the leading edge of the moving heating torch, where temperature gradient is much greater. At the tail of the moving heating torch, the converse feature is observed.

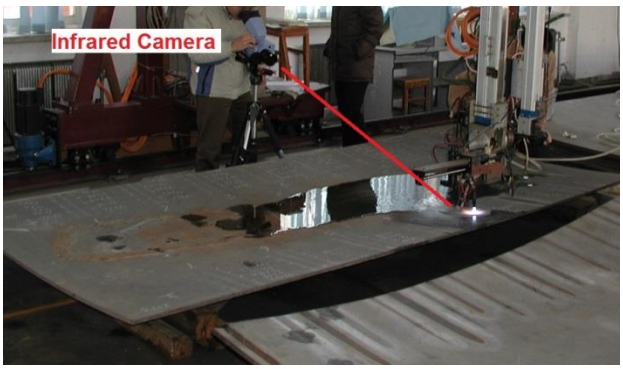

Figure 4. Experiments of line heating process

Figure 7 shows the comparison of the experiment and numerical temperature results. It can be seen from Figure. 7 that very good agreement between the numerical and experimental results has been achieved. The excellent match in the overall trends and peak values provides proof that the numerical model for the thermal problem is valid and could simulate the line heating process very well.

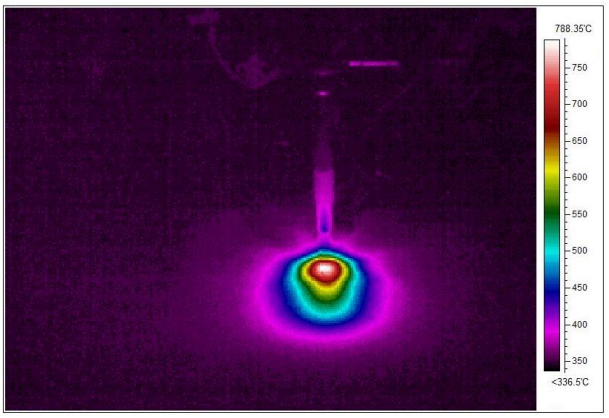

Figure 5. Experimental temperature field measurement with Infrared thermograph

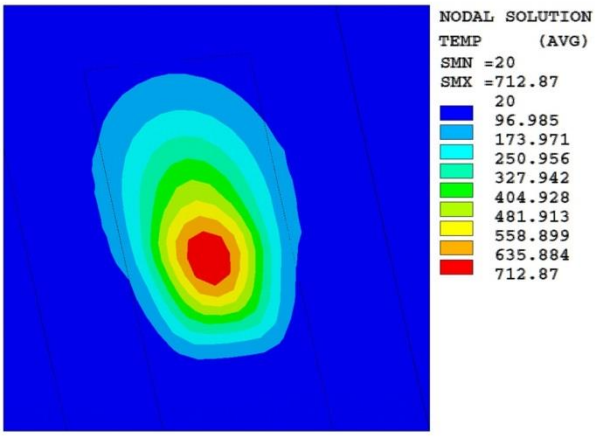

Figure 6. Numerical results of temperature fields

The shrinkages on the top surface were measured in experimental and numerical analysis. Surface shrinkage is the displacement between test points on the both side of the heat line after line heating process. There are five pairs of test points arranged evenly along the heating lines. Taken the No. 4 heating line as an example, Figure 8 shows the shrinkage curves in the direction of the heating line. It can be seen that most of numerical results agreed well with the experimental results with a variation of 5-10%. For all practical purposes and the tolerance achievable in a shipyard fabrication process, including the line heating process, precision of shrinkage measurement is about 0.5 mm. Therefore one would realize that the values of the shrinkage reported in the numerical and experimental results are basically the same.

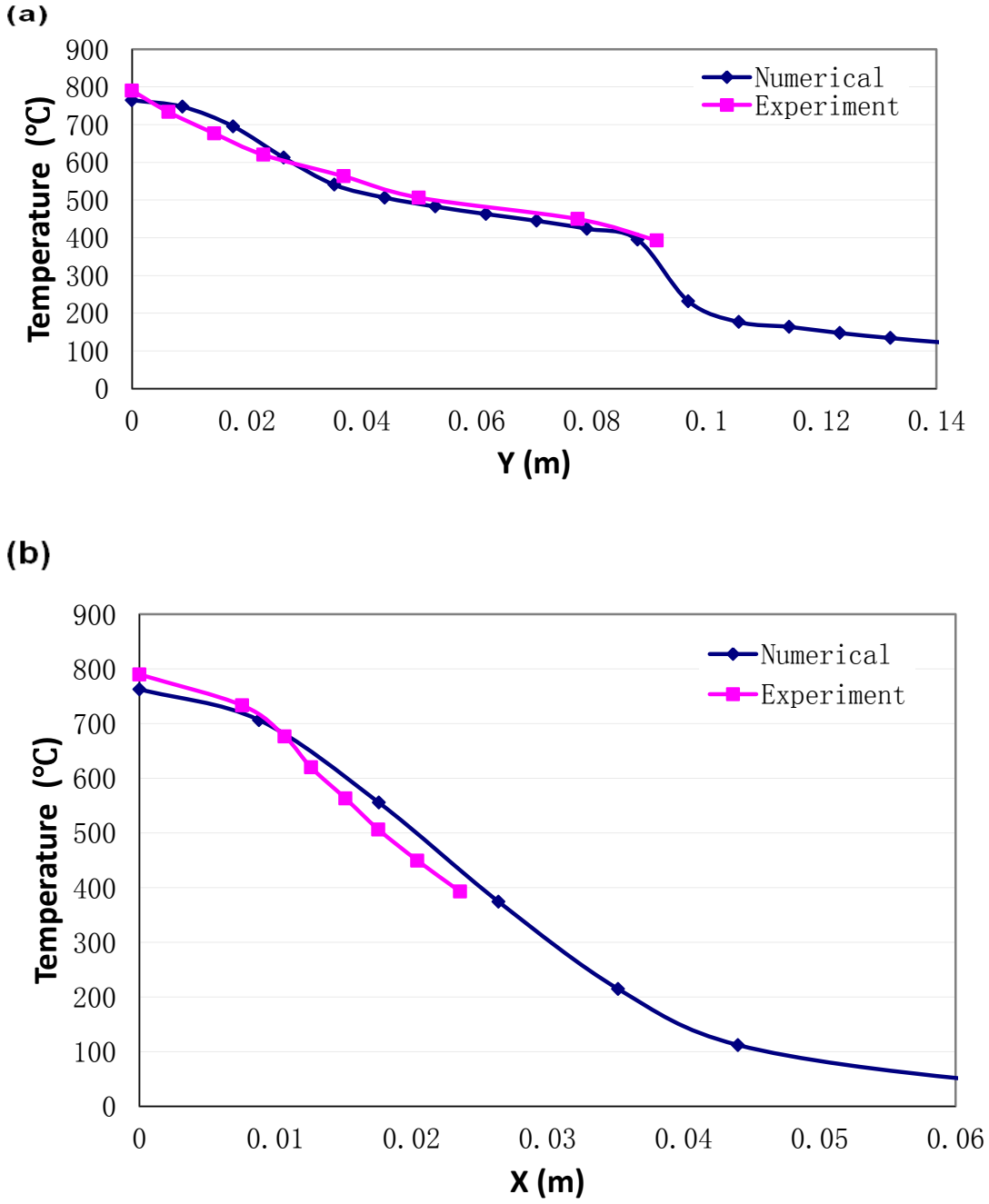

Figure 7. Comparison of the numerical and experiment results ((a): Results along heating line; (b): Result perpendicular to the heating line)

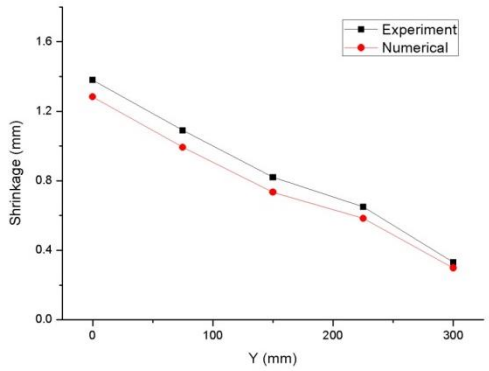

Figure 8. Shrinkage curves of the No.4 heating line

The distribution of residual stress on the top surface was also measured using the impact-indentation method. The change in strain, the so-called overlap strain increment, caused by an indentation was measured using a biaxial strain-gage Type BE120-3BA. Figure 9 depicts the distribution of residual stress in the Z-direction on the top surface, as measured by using the impact-indentation method and the simulated results using the finite element method.

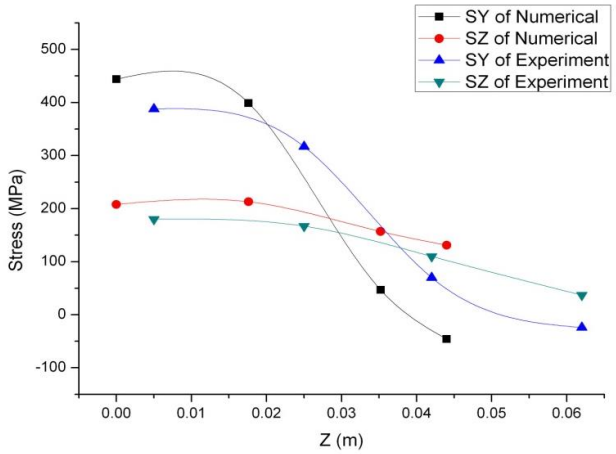

Figure 9. Comparison of longitudinal residual stress along the X direction

As can be seen in Figure 9, the simulated results depicted a slight incremental stress compared to the experimental results some distance away from the heat-line, but were almost identical near the heat line area. However, it is also seen that beyond the peak temperatures, the simulated SY stress along the z-direction decrease faster than the measured stress. Despite this discrepancy, the simulated and measured residual stress distributions agreed very well.

The temperature, residual deformation and stress distributions obtained through numerical analysis and those obtained from experimental measurements agreed well. These observations showed that the numerical model is valid.

3. NUMERICAL RESULTS AND DISCUSSIONS

3.1 RESIDUAL DEFORMATION DISTRIBUTION

The measurement points are five pairs of test points arranged evenly along the heating lines. The shrinkage results are shown in Tables 1 and 2.

Table 1. Numerical results of surface shrinkage on upper edge (mm)

Measure points	No.1	No.2	No.3	No.4	No.5	No.6	No.7
1	1.326	1.294	1.286	1.283	1.286	1.293	1.327
2	1.007	0.995	0.993	0.993	0.956	0.995	1.007
3	0.741	0.734	0.734	0.734	0.734	0.734	0.741
4	0.577	0.585	0.584	0.584	0.584	0.585	0.578
5	0.282	0.299	0.298	0.298	0.299	0.299	0.282

Table 2. Numerical results of surface shrinkage on lower edge (mm)

Measure points	No.8	No.9	No.10	No.11	No.12	No.13	No.14
1	1.681	1.678	1.690	1.694	1.690	1.676	1.681
2	1.272	1.295	1.314	1.320	1.314	1.294	1.273
3	0.895	0.906	0.916	0.919	0.916	0.905	0.895
4	0.678	0.690	0.691	0.691	0.691	0.690	0.679
5	0.327	0.351	0.350	0.350	0.350	0.351	0.328

It can be seen from Tables 1 and 2 that the shrinkages on either upper edge or lower edge of steel plate were symmetrical about the middle heating lines (No.4 and No.11). The reason for this is the boundary condition was symmetrical about the same axes. Taking the accuracy as 0.1mm, the shrinkage of each heating line were essentially the same. In other words, for all practical purposes, the final shrinkages for all the heating lines were the same. It could be seen that the shrinkages were not affected by the location when the process parameters were the same. They were basically localized deformations which were the result of the designed line heating process. It could also be seen that the shrinkages of the lower edge were slightly larger than the values of upper edge, even with the same process parameters. The shrinkages of the lower edge were affected by the heating process of the upper edge.

3.2 RESIDUAL STRESS DISTRIBUTION OF HEATING REGION

Figure 10 shows SY stress (stress along the Y-axis) contours corresponding to No.4 heating line on the upper edge. This study selected 5 points which were evenly distributed on the center of heating line. The distance between the selected points was 0.075m. The stresses at the selected points are shown in Figure 11.

It could be seen in Figure 10 that the highest stress location is mainly located at the line-heating line. Figure 11 (a) shows that the SY stress on the heating line is mainly tensile stresses and the magnitudes are much higher than the SZ stress (stress along the Z-axis). At the start and end points, the SZ stresses are compressive. At the mid-point of the heating line, the SZ stress is tensile. The SX stress is small and could be ignored.

It can be seen in Figure 11 (b) and Figure 11(c) that the stress distributions of No.1 and No.7 heating lines are essentially the same, and are slightly different from those of heating lines No.2 to No.6. The reason is that the boundary conditions were different. Whereas there was one heating line on one side of No.1 and No.7, there were 2 heating lines on either side of lines No.2-6. The stresses of No.4 and No.11 are shown in Figure 11 (d) in which No.4 and No.11 heating lines were the middle heating lines at the upper and lower edges, respectively. Heating Line No 4 showed slightly higher SY stress. Heating Line No 11 showed higher SZ stress at the edge of steel plate and lower away from the edges. Although the boundary conditions of the upper and lower edge were the same, the heating sequence was different and the process at the upper edge had an impact on the stress distribution at the lower edges.

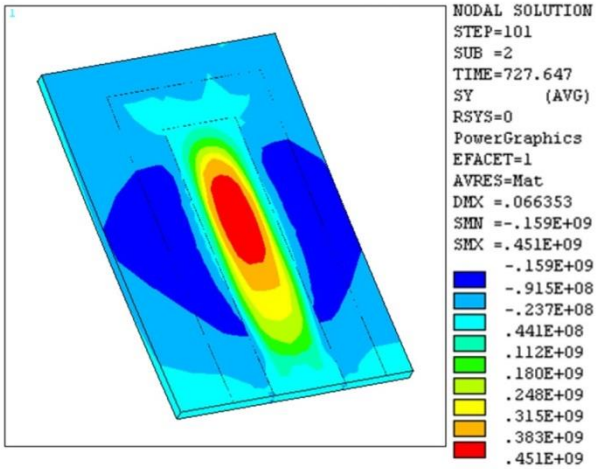

Figure 10. SY stress contours of No.4 heating line on the upper edge

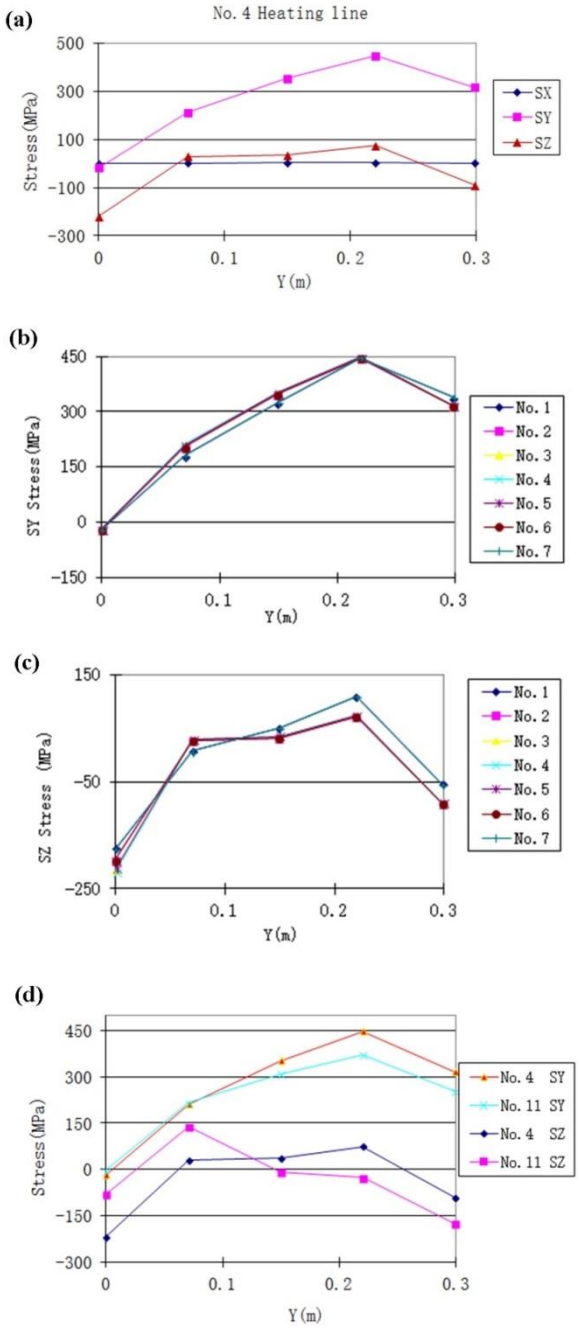

Figure 11. Stress distributions along heating lines. (a) Stress of No.4 heating line; (b) SY stress of No.1-No.7; (b) SZ stress of No.1-No.7; (d) Stress of No.4 and No.11.

Figure 12 shows the SX stress at heating line No.4 along the thickness direction. The study used 4 points which were evenly distributed on the edge of the steel plate are selected to illustrate the patterns of distribution of stress on the plate. The stresses of on the selected points are shown in Figure 13.

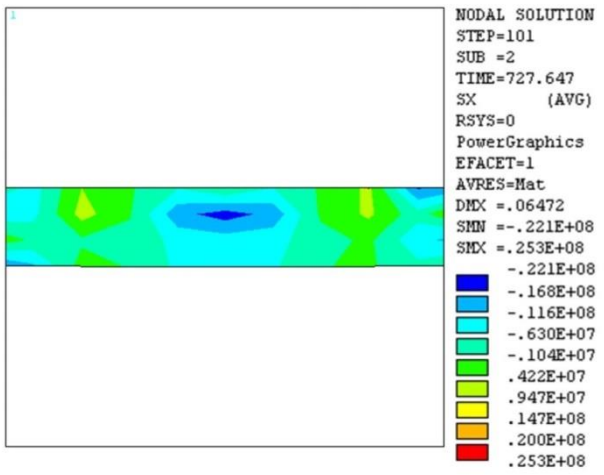

Figure 12. SX stress of No.4 heating line along thickness direction

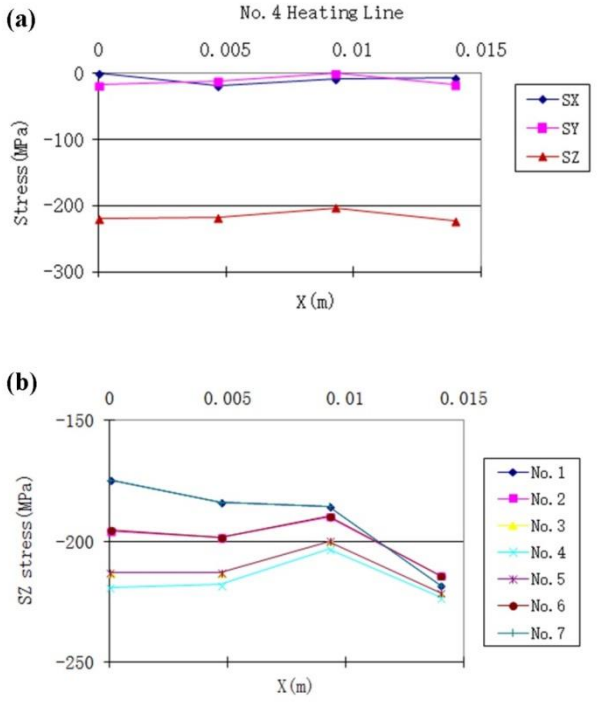

Figure 13. Stress along thickness direction. (a) Stress of No.4; (b) SZ stresses of No.1-No.7

It can be seen in Figure 12 that the SX stress is compressive below the heating line. Figure 13(a) shows that the stresses were stable along the thickness direction. The SX and SY stresses were low, and were about 10MPa. The SZ stress was higher, at about 210Mpa. Figure 13(b) shows the SZ Stress along the thickness at No.1 to No.7 heating lines. The stress distribution and the trend of variation for line No.1-No.7 were similar. The magnitude at line No.4 was the lowest, while the magnitudes for No.1 and No.7 were the highest.

3.3 RESIDUAL STRESS DISTRIBUTION OF THE WHOLE STEEL PLATE

Figure 14 shows the residual SY and SZ stress contour of the whole steel plate. Figure 15 shows selected curves on the upper surface of the steel plate. AB is the line on the surface of the lower edge. EF is the center line on the surface along the length direction. HG is the center line on the surface along the width direction. Figure 16 shows the stresses distribution on those lines.

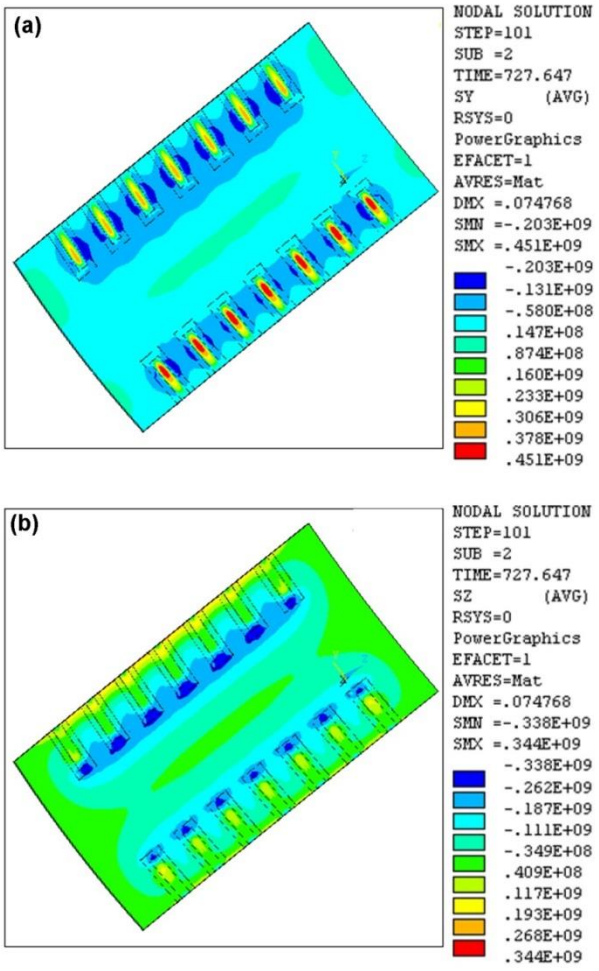

Figure 14. Stress contours in the whole steel plate: (a) SY stress and (b) SZ stress

It can be seen from Figure 14 that locations of large stress gradient were observed in the vicinity of the heated lines. The SY stresses on the heating lines were tensile and compressive between heating lines. The SZ stress in the middle of the steel plate was compressive and the largest value was observed near the start point of heating line.

As can be seen in Figure 16 (a) stress on line AB, SZ stress was mainly positive (tensile) in the heated region, and was negative (compressive) at the center of heating lines. The SY stresses were less than 50MPa. The non-heated region experienced compressive stress while

it was tensile stress on the heating line. The SX stress was much smaller in magnitude and might be ignored.

It could also be seen in Figure 16 (b) that the stress on line EF was much lower than the others as it was farthest from the heated zone. The SZ stress was about 30MPa and SY stress was about 20 MPa. The SX stress was too small which could be ignored. The SZ stress along the line was compression stress while the SY stress was tensile stress.

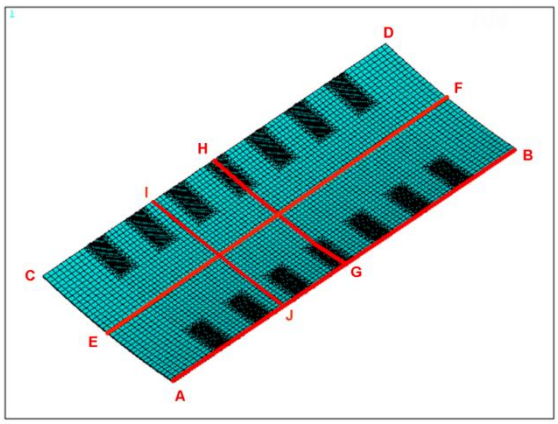

Figure 15. The selected lines on the upper surface of steel plate

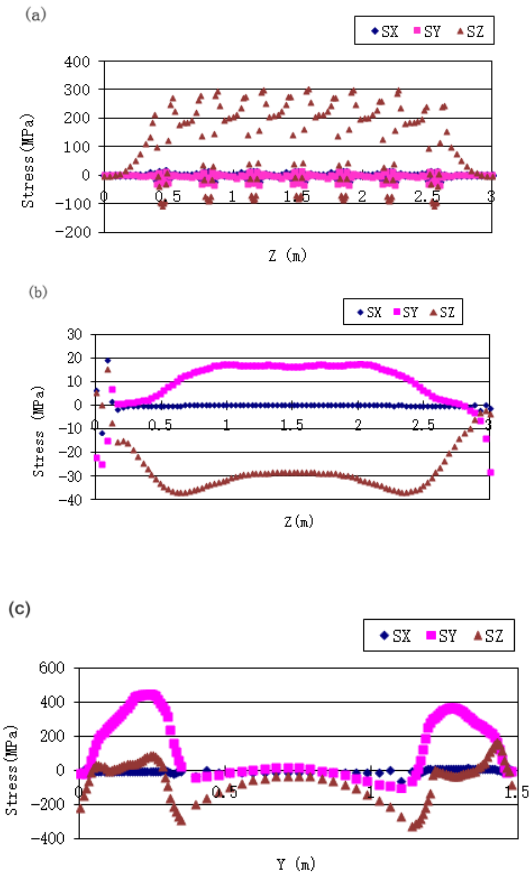

Figure 16. Stress distribution on the lines of (a) AB, (b) EF and (c) HG

It could be seen from the Figure 16 (c) that stress on line HG that SY stress at the heated region was high, and was tensile. The SY stress of non-heated region was mainly tensile stress. The SZ stress of heated region was tensile and compressive at the non-heated region. The peak value was observed near the heating line.

3.4 STRESS DISTRIBUTION AFTER UPPER EDGE PROCESSING

Figure 17 shows the residual SY and SZ stress contour distribution for the whole steel plate after the heating process at the upper edge. As shown in Figure 22, IJ was the line between two heating lines along the width direction at ¼ of the length. Figure 18 and Figure 19 show the stresses distribution on those lines.

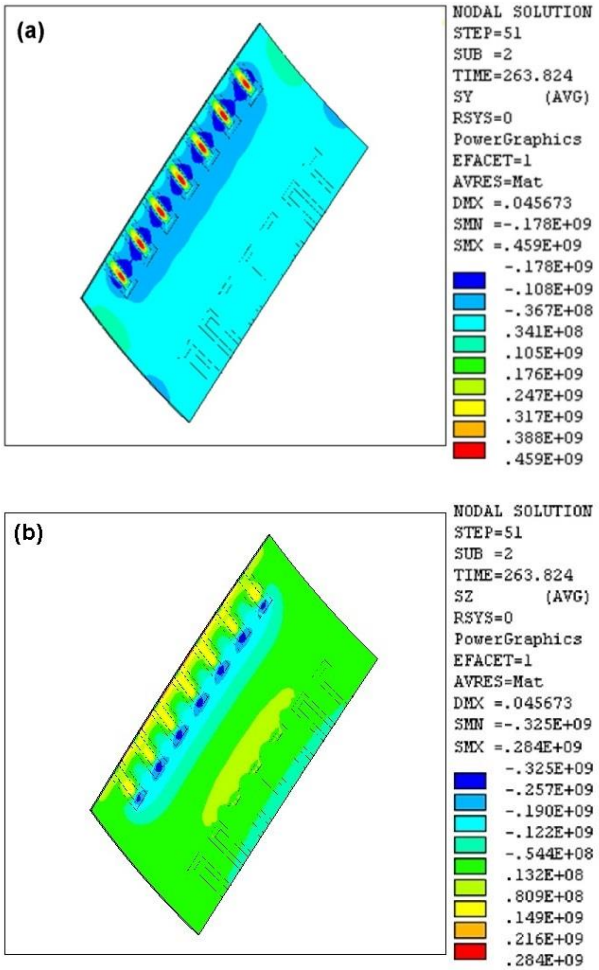

Figure 17. Stress contours after upper edge process. (a) SY stress and (b) SZ stress.

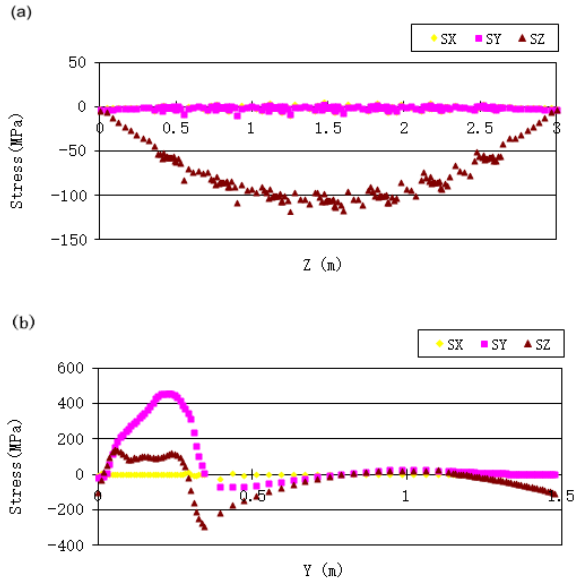

Figure 18. Stress distribution on the lines of (a) AB and (b) GH

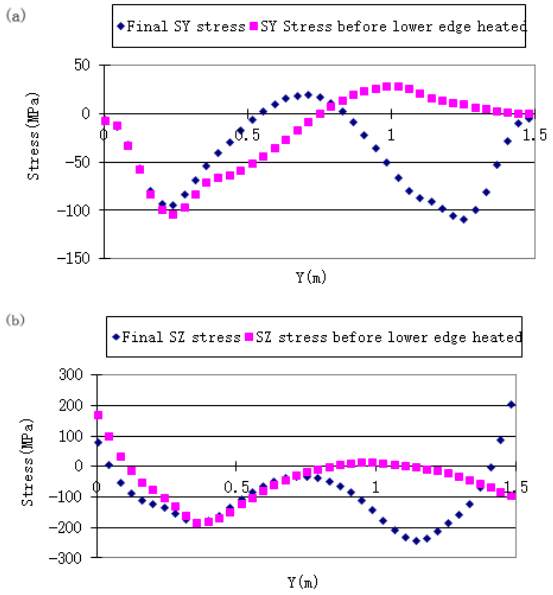

Figure 19. Line IJ Stress curves before or after process of lower edge: (a) SY stress and (b) SZ stress

It can be seen from Figure 17 (a) that SY stress was mainly localized on the upper edge area. The lower edge was generally not affected. From the results shown in Figure 17 (b) and Figure 18 (a), one can deduce that stress on the lower edge became compressive after the upper edge was heated. The largest stress was about 120MPa. The SX and SY stress at the lower edge (line AB) were small and could be ignored. The stress on line GH is also shown in the Figure 18 (b). The SZ stress at the heated region was positive (tensile). The stress at the lower edge was negative (compressive). The SY stress was tensile near the heating zone; SY stress at the lower edge was small and could be ignored. As can be seen from Figure 18, the heating process on the upper edge created compressive SZ stress at the lower edge.

The phenomenon may be explained as follows. The line heating process results in local shrinkage of the steel plate. Those local shrinkages at the heated lines create global deformation of the whole steel plate to achieve the targeted bend and curvature. This global deformation also results in residual stress at non-heated area in a steel plate. That is why the heating process at the upper edge creates compressive stress at the lower edge. This phenomenon also explains the observed results as shown in Tables 1 and 2 that shrinkages at the lower edge were larger than those at the upper edge. When the number of heating lines and the heating duration increase on the upper edge, the total shrinkage and deformation increase also. As a result, the compressive stress at the lower edge also increases correspondingly.

Figure 19 shows the stress differential at line IJ before and after the heating process at the lower edge. It could be seen that the peak value of the SY stress did not decrease after the heating process was performed at the lower edge. The final SY stress distribution at Line IJ was basically symmetrical about the center line.

It is also clear that the heating process at the lower edge will reduce the magnitude of the SZ stress at the upper edge. It means that the process of lower edge would also create compression stress at the upper edge. The final SZ stress at the lower edge was slightly higher than that at the upper edge. The final SZ stress at Line IJ was symmetrical about the center line.

4. CONCLUSIONS

A numerical study to analyze the residual stress distribution in the whole steel plate for line heating process had been performed. Based on the findings of the studies, the following conclusions are obtained:

- The line heating process has been adopted in shipbuilding and found to be a reliable process. So the residual stress level following a line heating process, especially the global stress level among the whole steel plate, could be used as a benchmark for plate bending process in the shipbuilding industry. It could be seen that the global stress could be as high as 120MPa at non-heated area in the line heating process.
- From the findings of the numerical analysis, one may deduce that the shrinkage at the lower edge was slightly larger than that at the upper edge. This conclusion is consistent with reported experimental studies. It is also concluded that the heating process at the upper edge will create compressive load at the lower edge. The compressive load would increase the shrinkage during line heating process.

5. ACKNOWLEDGEMENTS

The authors acknowledge the support of the CAM Lab, Department of Naval Architecture, Dalian University of Technology, Dalian, China.

6. REFERENCES

1. BRICKSTAD B., JOSEFSON B.L., 1998. A parametric study of residual stresses in multi-pass butt-welded stainless steel pipes, International Journal of Pressure Vessels and Piping, 75(1):11-25.
2. DENG D., 2009. FEM prediction of welding residual stress and distortion in carbon steel considering phase transformation effects, Materials & Design, 30(2):359-366.
3. JI, Z.S; LIU, Y.J., 2001. Development of study of ship hull plate banding by line heating. Journal of Dalian University of Technology, 41(5):505-510.
4. LIU, Y.J.; GUO, P.J., JI, Z.S., DENG, Y.P., 2006. Investigations of technique parameter prediction method of line heating based on genetic algorithm. Journal of Dalian University of Technology, 46(2):235-240.
5. JANG, C. D., SEO, S., AND KO, D. E., 1997. A study on the prediction of deformations of plates due to line heating using a simplified thermal elasto-plastic analysis. Journal of Ship Production, 13(1):22-27.
6. JONG, G. S., JONG, H. W., 2003. Analysis of Heat Transfer Between the Gas Torch and the Plate For the Application of Line Heating. Journal of Manufacturing Science & Engineering, 125(4):794-800.
7. MOSHAIOV, A. AND SHIN, J. G., 1991. Modified strip model for analyzing the line heating method-part 2: Thermo-elastic-plastic plates. Journal of Ship Research, 35(3):266-275.
8. MOSHAIOV, A. and VORUS, W. S., 1987. The mechanics of the flame bending process: Theory and applications. Journal of Ship Research, 31(4):269-281.
9. TENG T., FUNG C., CHANG P., YANG W., 2001. Analysis of residual stresses and distortions in T-joint fillet welds. International Journal of Pressure Vessels and Piping, 78(8): 523-538.
10. TOMITA, Y., OSAWA, N, HASHIMOTO K., SHINKAI N., SAWAMURA J., MATSUOKA K., 2001. Study on Heat Transfer Between Gas Flame and Plate During Line-Heating Process. Proceedings of the Eighth International Symposium on Practical Design of Ships and Other Floating Structures, 2001, Location: Shanghai, China
11. RADAJ D., Heat Effects of Welding: Temperature Field, Residual Stress, Distortion, Springer, 1992.
12. UEDA K., MURAKAWA H., RASHWAN A. M., OKUMOTO Y., and KAMICHIKA R., 1994a. Development of computer-aided process planning system for plate bending by line heating (report 1) – relation between final form of plate and inherent strain. Journal of Ship Production, 10(1):59-67.
13. UEDA K., MURAKAWA H., RASHWAN A. M., OKUMOTO Y., and KAMICHIKA R., 1994b. Development of computer-aided process planning system for plate bending by line heating (report 2) – practice for plate bending in shipyard viewed from aspect of inherent strain. Journal of Ship Production, 10(4):239-247.
14. UEDA, K., MURAKAWA, H., RASHWAN, A. M., OKUMOTO, Y., and KAMICHIKA R., 1994c. Development of computer-aided process planning system for plate bending by line heating (report 3) – relation between heating condition and deformation. Journal of Ship Production, 10(4):248-257.
15. YU, G, MASUBUCHI, K., MAEKAWA, T., PATRIKALAKIS, N.M., 1999. A finite element model for metal forming by laser line heating. In: Chryssostomidis C, Johansson K, editors. Proceedings of the 10th International Conference on Computer Applications in Shipbuilding, ICCAS '99, 2:409-418.
16. YU, G.,2000. Modeling of shell forming by line heating. Ph.D. thesis, Massachusetts Institute of Technology, Cambridge, MA.
17. YU, G., ANDERSON, R.J., MAEKAWA, T., PATRIKALAKIS, N.M., 2001. Efficient Simulation of Shell Forming by Line Heating. International Journal of Mechanical Sciences, 43(10):2349-2370.
18. ZHOU, B., LIU, Y. and TAN, S., 2014a. Numerical and experimental study on plate forming using the technique of line heating. International Journal of Maritime Engineering, 156(3):265-275.
19. ZHOU B., TAN S. and LIU Z., 2014b. Study on plate forming using the line heating process of Multiple-torch. Journal of Ship Production and design, 30(3):142-151.
20. ZHOU, B., LIU, Y.J., JI, Z.S., 2009. Numerical and experimental investigations on Temperature and stress distribution in oxygen cutting. Journal of Ship Production, 25(1): 14-20.
21. ZHOU, B., LIU, Y.J., TAN S.K., 2013. Efficient simulation of oxygen cutting using a composite heat source model, International Journal of Heat and Mass Transfer, 57(1):304-311.

